Assessing the geospatial nature of location-dependent costs in installation of solar photovoltaic plants

Basu, Soumya; Ogawa, Takaya; Okumura, Hideyuki; Ishihara, Keiichi N.

Energy Reports 7 (2021) 4882–4894

Contents lists available at ScienceDirect

Energy Reports

journal homepage: www.elsevier.com/locate/egyr

Research paper

Assessing the geospatial nature of location-dependent costs in installation of solar photovoltaic plants

Soumya Basu *, Takaya Ogawa, Hideyuki Okumura, Keiichi N. Ishihara

Graduate School of Energy Science, Kyoto University, Yoshidahonmachi, Sakyo-ku, Kyoto 606-8501, Japan

ARTICLE INFO

Article history:
Received 28 March 2021
Received in revised form 5 July 2021
Accepted 23 July 2021
Available online 9 August 2021

Keywords:
Solar photovoltaic
Location-dependent costs
Geospatial
Hedonic regression
Spatial optimization
Global optima

ABSTRACT

A major hurdle in increasing the economic feasibility of solar photovoltaic (SPV) plants is the ever-increasing share of location-dependent costs (land, transmission, labor, etc.) in total installation costs. Such costs are geospatial in nature, due to spatial socio-economics affecting them. Present geolocation methods, for locating SPV installation sites, do not consider the effect of location-dependent costs in installation. We use a spatial parameterization model for examining the factors causing spatial variation of the installation costs of land, labor, transmission and supply chains for suburban SPV plants, within a geographic boundary. The model is applied to Kolkata city, India, and the spatial variation of the costs are checked in a 2500 km^2 suburban boundary. The spatial variation of the location-dependent costs is mainly caused by the distance from an economic focal point of the city. The variations significantly optimize at minima points in the 2500 km^2 boundary, where the location-dependent costs increase by 10% with an average 2.6 km deviation and an average 6.7 km deviation from the global minima, for small and large plants, respectively. The spatial minima is mainly caused by variance of land and transmission costs. This minima location lies on the extrapolation of a line that connects the city focal point with the substation. The capacity of the SPV plants at the optima increases with increasing transmission voltage (11 kV to 66 kV), ranging from 4 MW to 257 MW in the case-study (small to large scale), while the minima shift away from the city focal point (ranging 29 km to 48 km) with increasing capacity. This study provides a perspective on how the spatial variation of installation costs can play a role in the geolocation of SPV plants. Furthermore, the empirical and spatial variation of location-dependent costs can enable energy planners to evaluate the economic feasibility of solar power and promote better land-use near cities.

1. Introduction

While fossil fuel-based energy has enabled the industrial revolution, it has also posed the serious threat of climate change. A majority of total carbon dioxide (CO_2) emissions are a direct result of fossil fuel (coal, oil and natural gas) usage for energy production. Even though fossil fuels are a relatively cheaper source of energy production, the hazards of climate change have brought forward renewable energy (RE) sources, as low emission energy sources. Despite low efficiencies of RE sources, solar photovoltaic (SPV) technology has become highly cost-competitive with fossil fuel sources, better than other RE sources like wind and geothermal, in recent years. This is primarily due to technological development and the abundance of the resource (Amjad and Shah, 2020).

In order to increase the economic feasibility of SPV power plants, most existing studies focus on optimizing technology-related cost for solar modules. Rapid developing technology and diversified usage, such as in net-zero emission buildings (Singh and Das, 2020), solar collectors (Das et al., 2015), water desalination (Mostafa et al., 2020), etc., have enabled solar module prices to decrease in every market worldwide.[1] Advances in material science (such as novel fabrication techniques, solar cell design, semiconductor band-gap engineering, etc.) have increased the efficiency, as well as decreased the overall manufacturing cost of solar panels (Campbell et al., 2009; Tang et al., 2011; Asim et al., 2012; Tillmann et al., 2019). Design modifications of SPV plants, to maximize solar power generation, are also explored in various studies, which develop algorithms to analyze and model solar irradiation patterns for maximum system output (Joyce, 2012; Ali et al., 2016; Diab et al., 2021; Meng et al., 2021). This has led to

* Corresponding author.
E-mail address: soumyabasu@rocketmail.com (S. Basu).

[1] SPV Module Prices drop: https://www.iene.eu/irena-forecasts-59-solar-pv-price-reduction-by-2025-p2740.html.

https://doi.org/10.1016/j.egyr.2021.07.068

Table i
List of abbreviations in paper.

CO_2	Carbon Dioxide
RE	Renewable Energy
SPV	Solar Photo Voltaic
NREL	National Renewable Energy Laboratory
IRR	Internal Rate of Return
LCOE	Levelized Cost Of Energy
MCDM	Multi-Criteria Decision Making
AHP	Analytical Hierarchy Process
ANP	Analytical Network Process
ELECTRE	ELimination Et Choice Translating REality
GIS	Geographic Information Systems
MUFSP	MUlti-Factor Spatial Parameterization
ACSR	Aluminum Cable Steel Reinforced
CBD	Central Business District
OLS	Ordinary Least Squares
ANOVA	Analysis of Variance
LDC	Local Distribution Center

Table ii
List of variables and nomenclature.

C_{loc}	Total Location-Dependent cost for SPV installation
C_{land}	Land cost for SPV
C_{trans}	Transmission cost for SPV
$C_{u-labor}$	Unskilled labor cost for SPV
$C_{s-labor}$	Skilled labor cost for SPV
C_{sc}	Supply chain cost for SPV
c_{ckt-km}	Cost of transmission line per-km
L_{min}	Line-of-sight distance to nearest substation
P_{peak}	Peak capacity for SPV plant
V	Voltage of transmission line
R	Resistance per-km of transmission line
β_0	Constant term in Hedonic regression
β_i	Regression coefficient for social variables
β_j	Regression coefficient for spatial variables
X_i	Social variables in Hedonic regression for land cost estimation
X_j	Spatial variables in Hedonic regression for land cost estimation
ε_0	Error term in Hedonic regression
A	Area of an SPV plant
$I_{u-labor}$	Work intensity of unskilled labor
$I_{s-labor}$	Work intensity of skilled labor
W	Average daily wage of skilled labor
D_{cbd}	Distance from CBD to the SPV plant center
μ	Average mileage of personal vehicles
c_{fuel}	Cost of fuel in India
F_L	Total weight of material to be transported
D_{rail}	Distance traveled by rail for transporting material
D_{ldc}	Distance from LDC to SPV plant center, for transporting material

a tremendous decrease in hardware (module and inverter) costs for SPV plants.

However, the viability of SPV power plants is not limited to SPV technology advances. Often, the affordability of solar power, as a major energy source, depends on the costs that are not associated with SPV modules and inverters (REI, 2016). The National Renewable Energy Laboratory (NREL) identifies reducing non-technology related costs (e.g.: labor, land, interconnection to grid, supply chain and project-design costs) as the chief driver in reducing installation costs of residential and utility-scale SPV systems (Fu et al., 2018). In fact, with the constant decrease of hardware costs, the non-SPV technology costs of installation have gone up significantly (30%–40% of total installation costs) in countries like United States, India, Japan, etc. (Fu et al., 2018; UERC, 2019; Höller et al., 2019). For example, in a study for SPV economic feasibility in Turkey, land cost was proven to be a very influential factor (Ozcan and Ersoz, 2019).

These costs involve location-dependent costs that vary across different countries, and even different places, since they are mainly influenced by socio-economic factors that vary geospatially (Charabi and Gastli, 2011). In fact, these location-dependent costs can vary across a limited geographic area, such as within a city (variation of land prices in a city- (Ottensmann et al., 2008). Hence, the economic feasibility of installing SPV plants is inherently dependent on specificity of location, due to the spatial nature of the location-dependent costs in limited areas, affected by geospatial socio-economics.

In literature, various ideas have been introduced for reducing non-hardware costs of SPV, such as Internal Rate of Return (IRR) calculations (Darling et al., 2011; Zhang et al., 2015). With respect to labor costs, technology for reducing labor time has also been discussed (Morris et al., 2014). Levelized cost of energy (LCOE) reduction is also an idea heavily explored in studies (Padmanathan et al., 2017; El-Shimy, 2012). Siali et al. (2016) introduced a model for optimizing grid costs by determining optimal supply points. However, these studies do not consider the effect of geospatially varying socio-economic factors on location-dependent costs of SPV plant installation.

Geolocation studies on SPV plant installation are restricted to non-empirical methods. Guaita-Pradas et al. (2019) tried to incorporate macro-economic factors for location-based cost-optimization for SPV, but lacks an empirical approach to reduce installation costs. Janke (2010) used Geographic Information Systems (GIS) for locating suitable areas in Colorado based on installation costs and environmental factors while Chakraborty et al. (2015) used technical mapping for finding ground areas for SPV to meet the energy demand of a University, but these models do not explore how spatially varying socio-economic factors affect SPV installation costs. GIS studies have also been used to estimate the solar energy potential in different regions (Sun et al., 2013). Multi-criteria decision making (MCDM) has been widely used with GIS for site selection of SPV plants. Analytical Hierarchy Process (AHP) in the MCDM domain is used to weight various parameters in the GIS map layers, and based on ranking of the aggregated weights, a site is selected on a map (Haaren and Fthenakis, 2011; Charabi and Gastli, 2011; Rumbayan and Nagasaka, 2012; Chang, 2015; Amjad and Shah, 2020). The process of weighting or indexing parameters was explored in depth by Banerjee and Islam (2011). The most commonly used factors in the AHP ranking process for solar site selection are: irradiance, land-use, slope of land, presence of water bodies, social acceptance of solar energy, etc., where the algorithm for parameter optimization is often K-means clustering (San Cristóbal, 2012; Wu and Geng, 2014; Chang, 2015; Amjad and Shah, 2020). Although complex decisions are made simple, the biggest drawback of the AHP and related algorithms, like Analytical Network Process (ANP), Elimination et Choice Translating Reality (ELECTRE), is that the weighting of parameters is non-empirical and often arbitrary. The factors of irradiance and social acceptance vary across wide geographies, while the variation of socio-economic factors, that affect location-dependent costs (like labor and land costs), occur in much smaller geospatial boundaries. Such models are, thus, not suitable for inspecting the effect of geospatial variance of socio-economics on location-dependent costs, primarily because they lack an empirical approach.

From the research gaps presented above, it can be concluded that there is a need to analyze the socio-economic factors that vary the location-dependent costs in limited geographies, and empirically determine the impact of installation costs on the location for SPV plants. This study aims to analyze the factors that influence the total location-dependent costs, for SPV power plant installation, to vary within a limited area. This paper focuses on the suburban region of a city, as the limited geography where the costs vary. We inspect how the geographical demographics and the socio-economics of a city cause a geospatial variance of the costs of SPV installation in the suburbs of the city. Our motivation is to examine whether the location-dependent costs, of the suburban SPV plant, can be geospatially minimized, and

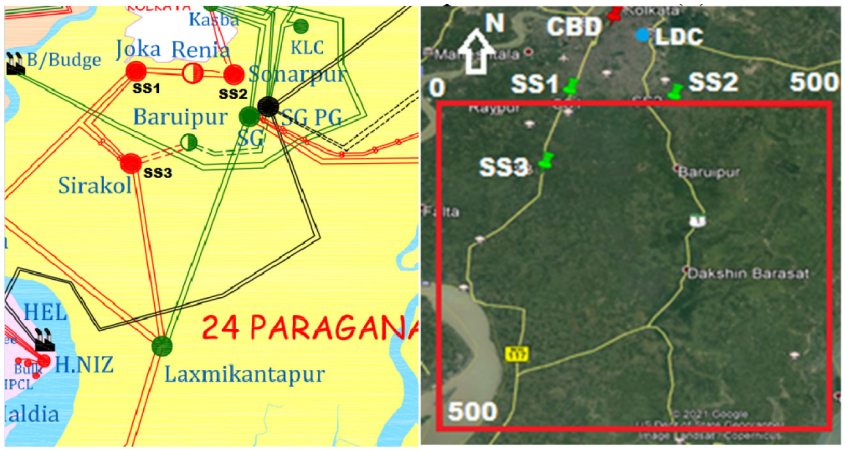

Fig. 1. The transmission network of Kolkata (*left*); 2500 km^2 simulation area divided into 500 × 500 mesh (Google Earth) with city center (CBD), local distribution center (LDC- the railway freight unloading station), and substations marked (*right*).

evaluate the primary factors that lead to the said minimization. Therefore, this study contributes to the assessment of economic feasibility of SPV power plants, close to a city.

Kolkata city,[2] India is used as a case-study, which makes a strong case for solar power. Kolkata, a growing metro city, aims to be a low-carbon city, but also poses a massive hike in power consumption from 2000 to 2025 (Figure 9 of Goulds-son et al., 2014). Simultaneously, India is a major solar energy player, ranking second in terms of SPV capacity added in 2018 (IRENA, 2019), which logically makes SPV power, the best option for future power generation in Kolkata. However, the share of land, labor and transmission costs to total installation costs, in India, has increased from 20% in 2010 to 40% in 2019 (CERC, 2010; UERC, 2019), and can become more than hardware costs, as module costs are becoming even cheaper (similar to that of United States: O'Shaughnessy et al., 2019). See Table i for the list of abbreviations in this study.

2. Methodology

The total cost function for installing a SPV plant may be written as in Eq. (1) below.

$$C_{tot}\,(x) = C_{loc}\,(x) + C_{non-loc} \tag{1}$$

where C_{tot} includes the total installation costs, C_{loc} are the location-dependent costs while $C_{\text{non-loc}}$ are the costs that are not spatially variable in a limited geography, and x represents a spatial influencing variable. Thus, the total costs are ultimately spatially dependent because of C_{loc}(x).

We use a multi-factor spatial parameterization (MUFSP) model involving GIS interface and statistical socio-economics to determine the location-dependent costs C_{loc}(x) for a suburban SPV plant installation, and how the costs vary across the suburban region of the city. Eq. (2) below represents the objective function of the MUFSP model, with the focus on land, transmission, labor, and supply chain costs, which are all spatial in nature, due to socio-economic and technical factors.

$$C_{loc}\,(x) = C_{trans}\,(x) + C_{land}\,(x) + C_{u-labor}\,(x) + C_{s-labor}\,(x) + C_{sc}(x) \tag{2}$$

where C_{trans} is the transmission cost, C_{land} is the land cost, $C_{\text{u-labor}}$ is the cost of unskilled labor while $C_{\text{s-labor}}$ is that for skilled labor, and C_{sc} represents the supply chain cost at the suburban location.

Each of the location-dependent cost functions are constructed based on relevant geospatial socio-economic parameters (x). These particular costs vary a lot within a limited geographical boundary, wherein in the next section we introduce the factors that lead to such variance. Using 3D simulation and GIS, the MUFSP model empirically determines each of the costs at every location, within the limited suburban boundary. The modeling problem is defined to identify which of the prime spatial factors (x) can minimize the total location-dependent costs C_{loc}(x). See Table ii for the list of variables used in the cost functions' construction.

3. Data and cost function construction

3.1. Simulation area

Fig. 1 represents the simulation boundary for the MUFSP model, for our case study of Kolkata. The simulation area is a squared 2500 km^2 area, south of the city of Kolkata. The northern and western suburban areas are heavily populated, while the eastern side is a marshy wetland, making these areas unsuitable for SPV plant development. In addition, Fig. 1 also shows the transmission network[3] around Kolkata, from which three representative substations (SS1, SS2 and SS3) are selected for the MUFSP model construction. The outer boundary of the simulation area (50 km from the edge of metropolitan Kolkata) is terminated at half the distance from the nearest city (100 km away from Kolkata- Mondal et al., 2018), as it is assumed that the spatial properties of socio-economic parameters beyond this distance will be affected by the factors of the other city, which is not considered in the model. The 2500 km^2 simulation area, programmed into MATLAB and SIMULINK R2016a environment, is divided into a 500 × 500 mesh (each element having a 100 m^2 resolution). Each of the 250,000-mesh elements is programmed to contain the objective function of Eq. (2), and the values are stored in the form of a 500 × 500 matrix [C_{loc}]. The existence of minimized cost locations is examined in this simulation area, for the location-dependent costs C_{loc}(x).

3.2. Transmission cost function (C_{trans})

The transmission cost function is composed of the various costs that are needed for joining a power supply source to the substation, which includes conductor, labor, grid upgradation and land-use costs as well as taxes associated with the costs. Table 1

[2] Kolkata Latitude and Longitude: https://en.wikipedia.org/wiki/Kolkata.

[3] West Bengal Power Transmission Map: W.B: http://www.wbsetcl.in/docs/power%20map.pdf.

Table 1
Details of the costs involved in per-km transmission line construction (extrapolated).

Cost Parameter	Costs (thousand INR[a])			
	11 kV	22 kV	33 kV	66 kV
Double Circuit ACSR Conductor	370	740	1450	2900
Bay Extension Land Cost at Substation	240	550	1060	2120
Control Panel and Feeder	390	620	1050	2100
Metering and Breaker	450	830	1300	2600
Total Cost per Circuit-km (c_{ckt-km})	1450	2740	4860	9720

[a] 1 INR = 0.013 USD (as of June 25, 2021).

Table 2
Details of the cross-sectional area and resistance of each transmission line.

Transmission voltage (kV)	Cross-section area (mm^2)	Resistance (Ω/km)
11	30	0.98
22	44	0.62
33	70	0.41
66	150	0.262

gives the benchmark costs for the Indian transmission network extension on a per-km basis (missing data is extrapolated from TSERC (2018)). Only 11 kV to 66 kV transmission lines are considered, because higher voltage lines are not feasible to support the intermittency of renewable energy sources like solar power.

Eq. (3) is the transmission line cost function for each element of the matrix [C_{loc}].

$$C_{trans} = c_{ckt-km} \cdot L_{min} \tag{3}$$

where c_{ckt-km} is the cost of transmission per km of a circuit (INR/km) (from Table 1), and L_{min} is the line-of-sight distance to the nearest substation from the mesh element (km).

Additionally, the peak-capacity of the SPV installation, centered at each point of simulation area, will be influenced by the voltage rating and properties of the transmission line. Aluminum Cable Steel Reinforced (ACSR) conductors are considered for the transmission lines at the voltage levels of 11 kV to 66 kV in Table 1 (Helioscart, 2020). The cross-sectional area of the transmission lines[4] influences the resistance of the line at each voltage level (Helioscart, 2020; Reta-Hernandez, 2006; UPPTCL, 2020). The details used in the modeling are shown in Table 2.

The resistances and the length of transmission line are used to calculate the peak-capacity at each mesh element for a given transmission line voltage (*equation (4) below*). The N-1 criterion is also considered, where a transmission line must be operated at less than 50% capacity, to support maintenance and as a fail-safe against one transmission line breakdown.

$$P_{peak} = \frac{V^2}{2(R * L_{min})} \tag{4}$$

where P_{peak} is peak capacity of SPV plant at each element of the mesh (MW), V is the maximum continuous operable voltage of transmission line (kV), and R is the resistance/km of the line (Ω/km). Thus, the capacity of the SPV plant is determined by the parameters and limitations of the transmission line, making the capacity endogenous in the model.

3.3. Land cost function (C_{land})

The land cost of the MUFSP model is guided by the principle of Hedonic pricing, which is an Ordinary Least Squares (OLS) regression model for determining property/land prices. Several studies have established the hedonic method as a means to estimate the land costs in urban and suburban areas, as a function of distance from the Central Business District (CBD) of a city along with other socio-economic predictors of land costs (Kain and Quigley, 1970; McDonald and McMillen, 1990; Ottensmann et al., 2008; Mondal et al., 2018). This is the first instance where the hedonic pricing model is used for a spatial optimization analysis that involves optimizing the installation costs of an SPV plant. Eq. (5) below represents the basic structure of the hedonic land cost function.

$$ln\,(C_{land}) = \left(\beta_0 + \sum_{i=1}^{n} \beta_i X_i + \sum_{j=1}^{m} \beta_j X_j + \varepsilon_0\right) \tag{5}$$

where C_{land} is a vector consisting of 141 samples of land prices, corresponding to municipal wards marked in Fig. 2[6], where the 1200 property price samples[7] from 141 wards are integrated into GIS interface (*Google Earth Pro 7.3.3*). Approximately 40% of the value of a property represents land price (Bourassa et al., 2011; Davis and Heathcote, 2007; Davis and Palumbo, 2008). The X_i is the n social variables interpreted from Indian census,[8] and X_j is the m spatial variables (distance and travel times) (Franklin and Waddell, 2003; Katz and Rosen, 1987) obtained using GIS tools. The β_0 is the intercept, the β_i and β_j correspond to regression coefficients for X_i and X_j, respectively, and ε_0 is the standard error for regression. All the socio-economic variables, for modeling the hedonic land cost function, are shown in Table 3, along with their mean and standard deviation.

The results of the hedonic regression model are tested with the Analysis of Variance (ANOVA) regression interface, and displayed

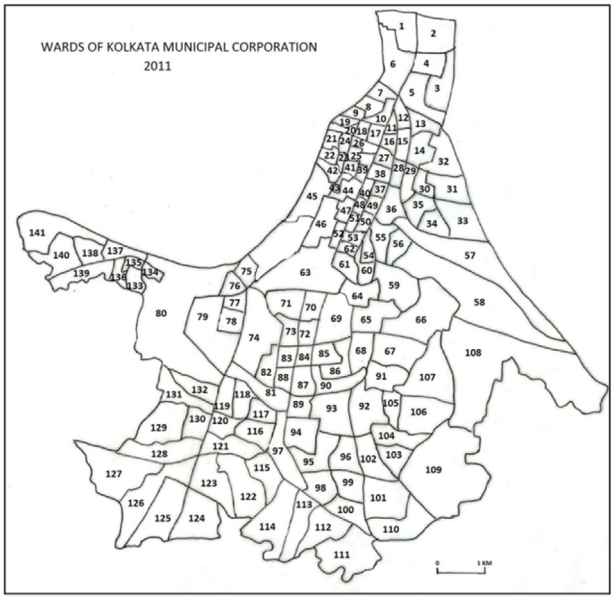

Fig. 2. Kolkata Municipal Ward map, with CBD marked (as dot).[5] Data pertaining to each variable of Table 3, from each of the 141 wards, is input into the hedonic model.

[4] Transmission Cables in Japan: http://www.hst-cable.co.jp/products/pdf/cableg3_2.pdf. (Accessed on Dec 10, 2020).

[5] Directorate of Census Operations, West Bengal: https://censusindia.gov.in/2011census/dchb/1916_PART_B_DCHB_KOLKATA.pdf.

[6] Kolkata Municipal Corporation Ward Data: https://www.kmcgov.in/KMCPortal/jsp/KMCWard.jsp.

[7] West Bengal Market Value of Land: W.B. Directorate of Registration and Stamp Revenue (Accessed on Dec 10, 2020): https://wbregistration.gov.in/(S(qxuw3khld42pbmhgt50xhpyz))/MV/MV_Land.aspx?type=L.

[8] Census of India 2011: https://censusindia.gov.in/DigitalLibrary/MFTableseries.aspx Historical census data of 2001: https://censusindia.gov.in/pca/pcadata/pca.html. (Accessed on Dec 10, 2020).

Table 3
The Hedonic Variables and their Means and Standard Deviations (*Please note that the equations for calculating the values of each variable is shown in Appendix A*).

Social variables (X_i)	Mean	Standard deviation
LN Land Cost (Dependent Variable)	7.664	0.612
Population Density (PD)	0.039	0.023
Sex Ratio (SR)	0.962	0.123
Literacy Rate (LR)	0.862	0.076
Female Literacy Rate (FLR)	0.866	0.077
Female to Male Lit Ratio (F-MLR)	0.954	0.108
Employment Rate (ER)	0.443	0.065
Female Employment Rate (FER)	0.25	0.095
Female to Male Emp Ratio (F-MER)	0.385	0.139
Youth Population Ratio (YPR)	0.063	0.022
Household Density (HD)	0.009	0.004
People per Household (PPH)	4.093	0.665
Spatial variables (X_j)	**Mean**	**Standard deviation**
Distance to CBD (D_{cbd})	5.415	2.587
Travel Time to CBD (TT)	27.87	11.22
Bus Time to CBD (BT)	55.62	25.79
Train Time to CBD (TRT)	40.87	21.25

Table 4
The Hedonic Land cost function result (*all the variables are significant at 1% level*).

Variables	Reg. coefficient	Standard error	*P*-Value
Intercept	10.018	0.227	0.000
Population Density (PD)	−4.082	1.328	0.003
Youth Population Ratio (YPR)	−4.725	1.331	0.001
People per Household (PPH)	−0.164	0.054	0.003
Radial Distance to CBD (D)	−0.08	0.029	0.007
Bus Time to CBD (BT)	−0.014	0.003	0.000
Pearson R: 0.88			
R-Square: 0.77			
Significant F: 0.00			

in Table 4 (*Please note that only the significant variables are shown, while the other hedonic models, that filter the insignificant variables, are in Appendix B*).

The land area, required by per unit peak-capacity of an SPV plant, is shown in Eq. (6) below (IRENA, 2014, *Page 12*- the standard area required by SPV plants according to latitude).

$$A = 0.0125 P_{peak} \tag{6}$$

where A (km^2) is the total SPV plant land-area with peak-capacity P_{peak}(MW) (*from* Eq. (4)).

The results of the hedonic pricing and the land area equation are then used to estimate the land cost, according to the peak-capacity of the SPV plant, at each point in the simulation area, which is shown in Eq. (7) below.

$$C_{land} = 134600 P_{peak} \cdot exp(10.018 - 4.082PD - 4.725YPR - 0.164PPH - 0.08D_{cbd} - 0.014BT) \tag{7}$$

where the other variables have their pre-established meanings. *Please note that km^2 is converted to ft^2, since the data of the dependent variable is in ft^2.*

3.4. Labor cost functions ($C_{u-labor}$ and $C_{s-labor}$)

The cost functions pertaining to labor costs are divided into: skilled labor and unskilled labor. The unskilled labor refers to the physical labor that is required in preparing the land, digging and drilling for the mounting structures, and the physical placement of the solar modules in the SPV plant. The skilled labor in SPV plant installation comprises the financial, legal, electrical, logistic and design experts who are involved during the actual project development and pre- and post-operations of installation. It is assumed that unskilled labor is hired locally at the suburban area where the SPV plant will be installed by the contractor in charge of SPV plant development. On the other hand, the skilled labor is assumed to be available in the metropolitan urban areas, and have to be transported to the site of the SPV plant development from the city by the contractor.

Table 5
The OLS (ANOVA) Regression results for daily Unskilled labor wage determination.

Variables	Reg. coefficient	Standard error	*P*-Value
Intercept	120.05	19.34	0.000
Male Literacy Rate (MLR)	229.60	18.82	0.000
Female Literacy Rate (FLR)	287.02	19.79	0.000
Male Employment Rate (MER)	319.13	22.27	0.000
Female Employment Rate (FER)	271.94	12.70	0.000
Pearson R: 0.97			
R-Square: 0.94			
Significant F: 0.00			

A study by Lillydahl and Singell (1985) examined how spatial variation of socio-economic factors (like employment and literacy rates) affect labor force participation. Rocha and Ponczek (2011) established that literacy and employment rates of an area, are key determinants for labor wages. The unskilled labor cost function is formed by an OLS regression model in Kolkata city, where the dependent variable is the daily wage of unskilled labor workforce, averaged for the 141 wards of Fig. 2 (data from Kolkata Municipal Corporation[9]). The independent variables are the corresponding literacy and employment rates of the 141 wards (data from Indian census [8]). The regression results are shown in Table 5. The Indian census data, for every village and town in the simulation area, is fed into the GIS interface based on the latitude and longitudes. A geographical moving average function establishes the literacy rate and the employment rate for each element of the simulation area, for estimation according to Eq. (8) below.

According to a study by Chandel et al. (2014), a total duration of 12 man-hours (1.5 to 2 man-days) of unskilled labor is required for installing 1 kW SPV plant peak-capacity.

$$C_{u-labor} = P_{peak} \cdot I_{u-labor}(120.05 + 229.60MLR + 287.02FLR + 319.13MER + 217.94FER) \tag{8}$$

where $I_{u-labor}$ represents the work intensity (days/MW) of unskilled labor required for installing a 1 MW peak-capacity SPV plant, and the other variables have their pre-established meanings.

The skilled labor cost function comprises: a. the daily wage of consultants (surveyed based on the popular employers in Kolkata, India[10]), since all the legal, financial, design and electrical experts are hired as consultants to solar construction projects; and b. the cost of fuel for transporting the skilled labor from the CBD to the site of SPV plant construction (since CBD is almost the geographical center of Kolkata – Fig. 2). The man-days of skilled labor are taken as 2120 days/50 MW, according to the Institute of Solar Technology,[11] India. It is also assumed that an expert would travel on a personal vehicle to the suburban site, and thus, fuel cost is calculated for twice the distance from CBD to the geolocated SPV plant site for each man-day of labor (data collected from GIS). Eq. (9) below, shows the skilled labor cost function for each point.

$$C_{s-labor} = P_{peak} \cdot I_{s-labor}(W + 2D_{cbd} \cdot \mu \cdot c_{fuel}) \tag{9}$$

[9] KMC Ward Income Data: https://www.kmcgov.in/KMCPortal/jsp/KMCPortalHome1.jsp .

[10] Average Salary of Kolkata: https://www.payscale.com/research/IN/Location=Kolkata-West-Bengal/Salary. (Accessed on Jun 10, 2021).

[11] Skilled Labor: https://institute-of-solar-technology.blogspot.com/2018/03/manpower-requirements-for-solar-pv.html.

where W represents the average daily wage (INR/day) for a skilled laborer, $I_{s-labor}$ is the work intensity (days/MW) of skilled labor for installing a 1 MW peak-capacity SPV plant, D_{cbd} is the distance (km) from CBD to a simulation area point (Table 3), μ is the average mileage[12]/fuel efficiency (km/liter) of personal vehicles in India and c_{fuel} is the cost of fuel[13] (INR/liter) in India.

3.5. Supply chain cost function (C_{sc})

For the purposes of modeling, it is firstly assumed that the solar modules, inverters and mounting structures are produced domestically in India and transported from Indian manufacturing plants. The first part of the supply chain cost is the cost involved in transporting the material, by railway network, from the manufacturing plant to the local distribution center. The second part of the supply chain is where the material is transported by road freight from the local distribution center (LDC) to the simulation area point where the SPV plant might be installed. Fig. 1 shows the location of the LDC. Table 6 shows the transportation distance and the total freight load of the material (obtained from Oguz and Şentürk, 2019), along with the assumed freight rates for both road and rail. Eq. (10) below, represents the supply chain cost function at each point of the simulation area.

$$C_{sc} = P_{peak} \cdot F_L(1.66D_{rail} + 12D_{ldc}) \tag{10}$$

where C_{sc} is the total supply chain cost (INR) at each point of simulation area according to peak-capacity P_{peak}, F_L is the load of material to be transported (ton/MW), D_{rail} is the distance by rail (km) according to Table 6, and D_{ldc} is the distance by road from the LDC to a simulation area point, where the SPV plant site will be centered.

4. Results and discussion

4.1. Existence of the optima

The variation of the location-dependent costs $C_{loc}(x)$, across the simulation area of 2500 km^2, is shown in Figs. 3 and 4. Fig. 3 shows the details of the costs when only substations SS1 and SS2 are considered. Fig. 4 shows the details of the costs considering all the three substations of SS1 to SS3. The direction of observation of the 3D visualization is from northeast of Fig. 1. It is found that, there exist optimized locations, in the suburban region, where the spatial variation of the total location-based SPV installation costs is minimum, for each level of transmission voltage. Table 7 corresponds to Fig. 3, where SS2 influences the optima. Table 8 corresponds to Fig. 4, where SS3 influences the optima.

The land cost exponentially decreases as the socio-economic determinants of PD, PPH, YPR and BT (Table 3) vary with distance from CBD (D_{cbd}). The cost of unskilled labor linearly decreases from the edge of the city due to decreasing employment and literacy rates as we move away from the city. The substations being located close to the city, transmission cost linearly increases with distance from the substation. Transportation cost of skilled labor and supply chain cost also increase with distances D_{cbd} and D_{ldc}, respectively. Thus, spatial socio-economic variances are primarily caused by distance from the city, which spatially varies the location-dependent costs in the suburban region.

It is observed, from Tables 7 and 8, that the total location-based costs, at the minima points, are lesser when SS3 is considered, for every level of transmission voltage. Thus, it can be inferenced that a substation farther away from CBD will always influence the global optimal cost location. However, the optimal locations associated with SS2 form a second, localized minima, which can be a second appropriate location for installing the suburban SPV plant.

4.2. Significance of the minima positions

Figs. 3 and 4 show a significant spatial variation of the costs in the 2500 km^2 suburban area. However, in order to test the significance of the minima $C_{loc}(x)$ locations, the cost variation in the immediate vicinity of the global minima (Table 8 and Fig. 4) is studied from the contour patterns. From Fig. 4, it is observed that the contour lines are more densely packed towards the substation and CBD, while the packing is less dense perpendicular to the substation and CBD. Therefore, Table 9 shows the minimum and maximum spatial deviations (in km) that are incurred, for $C_{loc}(x)$ to increase by 5% and 10% from the value at the global minima.

It can be ascertained that the minima are very sharply defined in the case of smaller SPV plants (11 kV case), which are closer to the CBD. As the transmission voltage (and SPV plant capacity) increase, the gradient of cost around the minima is less steep than that of smaller SPV plants, but the cost is still significantly optimized at the global minima. Thus, it can be said that geolocation is very sensitive for optimizing the location-dependent costs for a smaller SPV plant, and the sensitivity slightly decreases with increasing capacity. Any deviation beyond 4.6 km, 3.4 km, 2.5 km, and 1.6 km (average of the 5% cost increases in Table 9), in the 66 kV, 33 kV, 22 kV and 11 kV cases, respectively, will significantly raise the $C_{loc}(x)$ of the installation costs. This proves that the MUFSP model is important in the consideration for cost reduction/optimization of suburban SPV plants.

4.3. Variance of location-based costs at optima

Figs. 5 and 6 show the trend of the cost function variations at the minima for each voltage.

Land Cost: The 11 kV optimal locations, corresponding to small-scale P_{peak} of SPV plant and being closer to the city, are not economical due to higher land cost. The per unit land cost decreases by a factor of 6, from small- to large-scale SPV plant (4MW to 188MW), when serviced by SS2, and by a factor of 4 (6MW to 257MW), when connected to SS3. When the 11 kV line is considered, the position of the optimal location is much closer to the CBD for SS2, leading to a much higher per unit land cost than SS3. Interestingly, the difference of distance of the minima from CBD, between SS2 and SS3, reduce at higher voltages, resulting in comparable per unit land cost at 66 kV.

Transmission cost: The transmission cost reduces by a factor of nearly 2 in both cases, from 11 kV to 66 kV. At each voltage level, the transmission cost difference, between similar voltage levels for SS2 and SS3, is essentially double. This is particularly interesting when we realize SS3 is twice the distance from the CBD than SS2. We can conclude that the per unit costs of installation, for a suburban SPV plant, will be higher when connecting to a substation, closer to the city, due to a longer line of transmission. Even though the optima, associated with SS2 and SS3, lie almost at the same distance from the CBD for 22 kV to 66 kV, the peak-capacity of the plant at the optima is lesser with SS2, due to a longer transmission line offering greater resistance.

Labor costs: The ratio of land cost to total labor cost, at small-scale P_{peak} (4MW) is 5:1 for SS2 and 7:2 for SS3 (6MW). However, with larger capacity SPV plants (connected by 33 kV and 66 kV), the ratio of land cost to total labor costs become almost 1:1, with a higher share of labor costs. It is observed that with the increase in capacity, the per unit cost of unskilled labor decreases, while

[12] Average Mileage of Cars: https://www.olx.in/en/cars_c84/q-mileage. (Accessed on Jun 10, 2021)

[13] Fuel Price in India: https://economictimes.indiatimes.com/wealth/fuel-price/petrol. (Accessed on Jun 10, 2021).

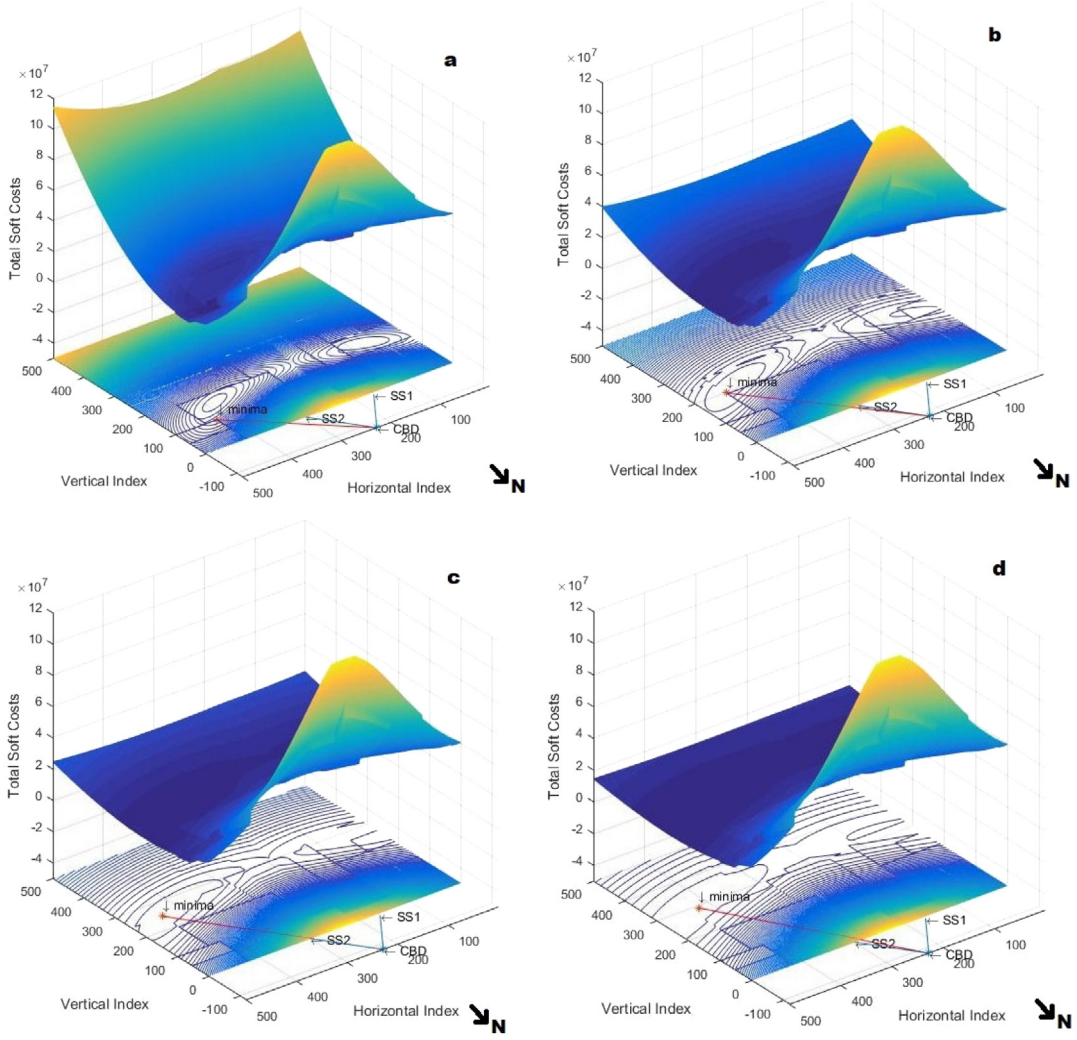

Fig. 3. The total cost variation in the 500 × 500 simulation area, considering SS1 and SS2 for (a) 11 kV, (b) 22 kV, (c) 33 kV, (d) 66 kV lines. Minima is mostly on extrapolated line from CBD to SS2.

Table 6
Assumptions for the supply chain cost function (*per 1 MW of capacity*).

Material	Freight load F_L (ton) per MW	Rail supply chain		Road supply chain	
		Distance D_{rail} (km)	Unit cost (INR/ton-km)	Distance D_{ldc} (km)	Unit cost (INR/ton-km)
Panels	77.85	1859[a]	1.66[b]	Variable	12[c]
Mounting Structure	9.48	1274[d]			
Inverter	18.5	1903[e]			
Total (Avg. Distance)	105.8	1814.3			

[a]Panel Manufacturer: https://www.adanisolar.com/.
[b]India Railway Freight Rates: https://www.statista.com/statistics/741428/india-railway-freight-rate-per-metric-ton.
[c]Truck Freight Rates: https://nationalfreightindex.co.in/. (Scaled up, as per short distance service).
[d]Mounting Structure Manufacturer: https://www.loomsolar.com/
[e]Inverter Manufacturer: https://thesunexchange.com/project.

Table 7
Characteristics of the Optimized Location, when substations SS1 and SS2 are considered. SS2 influences the Optimal Cost Location.

Trans Volt (kV)	Minima Dist. from CBD (km)	Minima Dist. from Substation (km)	Capacity (P_{peak}- MW)	SPV Land Area (A-km^2)	Land Cost (C_{land}- INR/MW)	Transmis-sion Cost (C_{trans}- INR/MW)	Skilled Labor Cost ($C_{s-labor}$- INR/MW)	Unskilled Labor Cost ($C_{u-labor}$- INR/MW)	Supply Chain Cost (C_{sc}- INR/MW)	Total Minima Cost (C_{loc}- INR/MW)
11	29.05	15.57	3.97	0.049	13.22×10^6	9.42×10^6	1.19×10^6	1.46×10^6	0.31×10^6	25.61×10^6
22	38.29	24.47	15.95	0.199	5.46×10^6	7.66×10^6	1.25×10^6	1.34×10^6	0.35×10^6	16.08×10^6
33	42.49	28.63	46.38	0.580	3.22×10^6	6.17×10^6	1.31×10^6	1.29×10^6	0.38×10^6	12.38×10^6
66	45.58	31.77	188.35	2.35	2.27×10^6	4.04×10^6	1.35×10^6	1.24×10^6	0.39×10^6	9.30×10^6

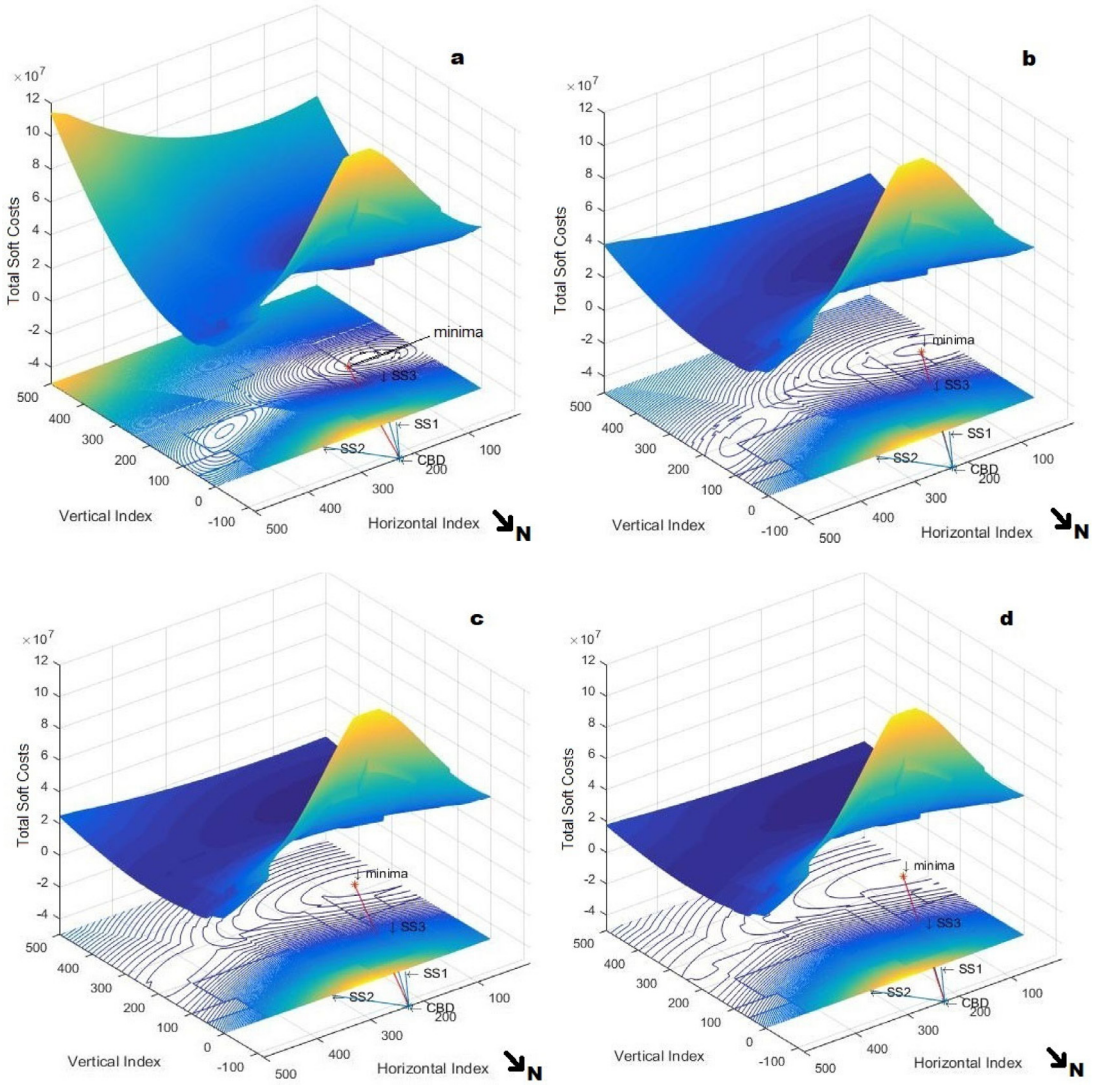

Fig. 4. The total cost variation in the 500 × 500 simulation area, considering SS1, SS2 and SS3 for (a) 11 kV, (b) 22 kV, (c) 33 kV, (d) 66 kV lines. Minima is mostly on extrapolated line from CBD to SS3.

Table 8
Characteristics of the Optimized Location, when substations SS1, SS2 and SS3 are considered. SS3 influences the Optimal Cost Location.

Trans Volt (kV)	Minima Dist. from CBD (km)	Minima Dist. from Substation (km)	Capacity (P_{peak}- MW)	SPV Land Area (A-km^2)	Land Cost (C_{land}- INR/MW)	Transmission Cost (C_{trans}- INR/MW)	Skilled Labor Cost ($C_{s-labor}$- INR/MW)	Unskilled Labor Cost ($C_{u-labor}$- INR/MW)	Supply Chain Cost (C_{sc}- INR/MW)	Total Minima Cost (C_{loc}- INR/MW)
11	34.07	11.14	5.54	0.069	8.22×10^6	4.83×10^6	1.22×10^6	1.33×10^6	0.32×10^6	15.91×10^6
22	40.56	17.14	22.76	0.285	4.07×10^6	3.77×10^6	1.28×10^6	1.27×10^6	0.35×10^6	10.76×10^6
33	45.56	22.24	59.70	0.746	2.25×10^6	3.72×10^6	1.32×10^6	1.21×10^6	0.38×10^6	8.88×10^6
66	47.57	24.36	257.3	3.22	1.78×10^6	2.53×10^6	1.35×10^6	1.20×10^6	0.41×10^6	7.29×10^6

Table 9
Distance from Global Minima where the cost increases by 5% and 10% (Fig. 4).

Transmission voltage (kV)	Spatial deviation from the global minima for cost increase from minima (km)			
	Cost increase by 5%		Cost increase by 10%	
	Minimum Dev.	Maximum Dev.	Minimum Dev.	Maximum Dev.
11	1.5	1.6	2.6	2.6
22	2.2	2.9	3.2	4.2
33	2.7	4.1	4.2	6.0
66	3.8	5.4	5.8	7.5

that of skilled labor increases, because of the relation of the cost functions to distance from the city.

The per unit labor costs do not vary as much with distance from the city, or with scale, as land and transmission costs (Figs. 5

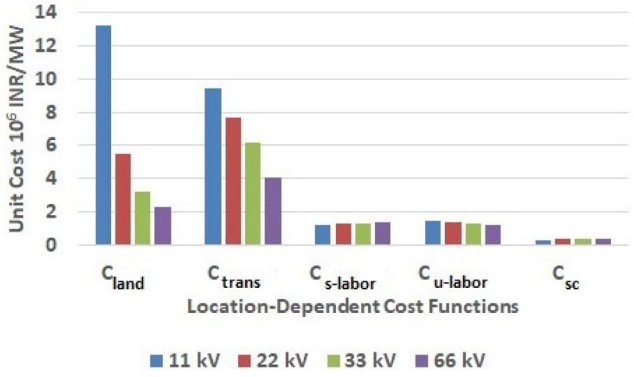

Fig. 5. Variation of the Location-Dependent Costs at the minima, when connected to SS2.

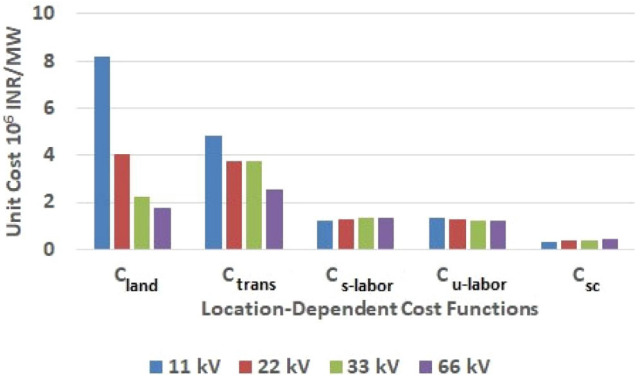

Fig. 6. Variation of the Location-Dependent Costs at the minima, when connected to SS3.

and 6). Also, the impact of the spatial variation of supply chain costs is negligible, on the optimal locations, compared to that of the other location-dependent costs. Moreover, the share of land and transmission costs vary from 60% (66 kV case in Table 8) to 88% (11 kV case in Table 7) of the total location dependent costs ($C_{loc}(x)$). Thus, the spatial nature of the land and transmission costs are the most sensitive factors for determining the position of the minima. In the cases of 11 kV to 33 kV transmission lines, land and transmission cost effect is magnified, creating a very sharp minima (Figs. 3 and 4). The minima are little less defined in the case of 66 kV lines, but still significantly caused by land and transmission costs.

4.4. Comparison of results with literature

The latest benchmark costs of India (UERC, 2019), estimates land cost at INR 5 million/MW, labor cost at INR 3.28 million/MW and transmission cost at INR 1.87 million/MW (total: INR 10.15 million/MW). In comparison with the results at the optima, it can be seen that transmission costs are higher than the benchmark estimates in suburban cases. However, the model provides an opportunity for an immense reduction in land cost and unskilled labor cost, as the results in the 33 kV and 66 kV are 1.5 to 2 times lesser than that of the benchmark estimates. We can infer, that overall installation costs are optimized with the spatial optimization model to be below the benchmark estimates, for suburban SPV plants between 50MW and 250MW. Chandel et al. (2014) designed an on-site SPV plant for Jaipur city, India; when comparing the land cost, it is seen that the estimates in Chandel et al. (2014) were much larger compared to the spatially optimized results, and thus, the importance of this model can be established. Our

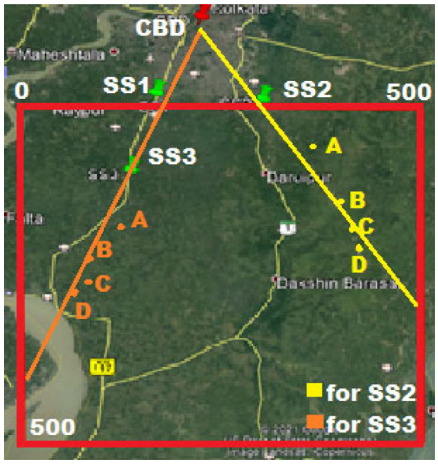

Fig. 7. The optimized cost positions with respect to Figs. 3 and 4, represented with the geolocation of the SPV plants marked. The minima points lie almost on the line extrapolated from the CBD to the substation. The minima move away from the CBD with increasing voltage and SPV capacity. (*Legend: 11 kV- A; 22 kV- B; 33 kV- C; 66 kV- D*).

results of the labor costs, however, agree with the estimates of *Chandel et al. (2014)*. In comparison with geolocation algorithms of MCDM methods (Amjad and Shah, 2020; Chang, 2015; Wu and Geng, 2014), our results provide a definitive outcome, where the installation costs are shown to vary geospatially, and are even optimized at a specific location within the limited geographic boundary of the suburban region of Kolkata city. The biggest difference between the MCDM geolocation and the spatial optimization model discussed here, is that the MCDM methods do not provide the effect of scale of the power plant on the geolocation, because MCDM algorithms do not empirically optimize location, based on costs.

5. Simplification of spatial optimization

The position of the optima shifts away from the CBD as the SPV peak-capacity increases. The shifting away of the optima from the CBD is more noticeable during changes at lower capacities (Tables 7 and 8) than at higher capacities. The optima also shift away by a greater margin with change in capacity, if the SPV plant, at the optima, is connected to a substation closer to the city. Fig. 7 shows that in all the cases, the optimum geolocations (for the cases in Tables 7 and 8) approximately lie on a straight line that connects the CBD and the substation, to which the optima are connected.

From the above paragraphs, it has been concluded that:

a. the distance from the city is the main cause for the spatial variation of location-dependent costs,
b. land and transmission costs mainly determine the position of the cost-optimized location, and
c. the optima lie on a straight line that connect the CBD and the substation.

Thus, the findings of this study can be simplified, as shown in Fig. 8 and Eqs. (11)–(13) below, for geolocating an SPV plant with minimum location-dependent costs, within a limited geography.

Ignoring the labor costs, supply chain cost, and PD-PPH-YPR-BT of land cost, the cost function $C_{loc}(x)$ for location-dependent cost optimization can be reduced to (*from* Eqs. (3) and (7)),

$$C_{loc}(D) = Ae^{-\alpha_1 D} + \alpha_2 L_{min} \tag{11}$$

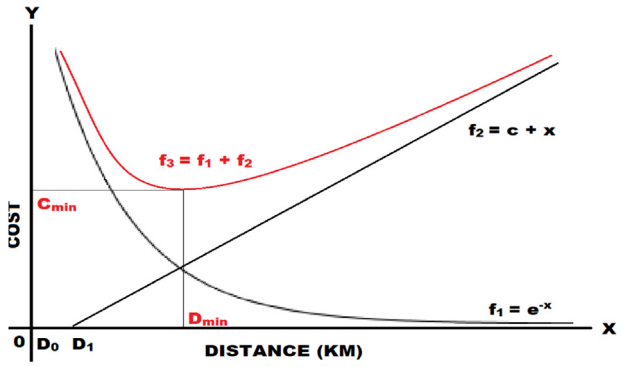

Fig. 8. (**Representative figure**) land cost f_1 decreases with distance from city CBD (D_0). With substation located at city boundary (D_1 km from CBD), transmission cost f_2 increases linearly. At location with distance $D_{\min}$ km from CBD, the total cost function f_3 will have minimum cost $C_{\min}$.

where α_1 is the per ft^2 land cost, α_2 is same as $c_{\mathrm{ckt-km}}$, A is taken from Eq. (6) (area of P_{peak} SPV plant), and C_{loc}(D) is total cost as a function of distance from CBD (D_{cbd}). Taking distance between CBD and substation to be a constant k,

$$C_{loc}(D) = Ae^{-\alpha_1 D} + \alpha_2(D - k) \tag{12}$$

Taking the first derivative of C_{loc}(D), the distance of the cost-optimized location from CBD is,

$$D_{min} = \frac{1}{\alpha_1} ln \frac{A\alpha_1}{\alpha_2} \tag{13}$$

The cumulative cost at the optima, according to the simplified model, can be found by substituting the value of $D_{\min}$ in Eq. (12).

A solar plant designer only needs to consider the extrapolation of a straight line for geolocating an optimized installation cost-location for a suburban SPV plant, wherein the line connects an economic focal point of a city (associated with land and labor costs) to the connecting substation. The position can be determined simply by the consideration of land and transmission costs (Eq. (13)). In essence, a three-dimensional problem (two spatial dimensions and one cost dimension) is reduced to a two-dimension problem (one linear and one cost dimensions) in optimization.

While the CBD is the focal point for both the land and the labor cost functions in this paper, the CBD may be modified to be any focal point of economic rationality, with respect to the socio-economics of a city. This case-study represents the outcome based on Kolkata city, India. In the case of suburban areas of countries with much higher land cost than India (such as U.S. and Japan), the optima will lie much farther away than the Indian case ($D_{\min}$ is directly proportional to product of unit land cost and SPV plant area- Eq. (13)). In such a situation, the initial simulation area needs to be larger for seeking the optima. With an increased distance from the focal point, the spatial variation of labor costs, may in such cases, become much more significant than the Indian case. However, with labor costs modeled from the same economic focal point as land costs, the optima will still lie on the extrapolation of the line connecting the focal point to the substation. The only change to Eq. (13) for adding labor costs, will be to add the per unit labor cost term to the natural logarithm denominator. With increasing per-km transmission costs, the optima will move closer to the focal point, according to Eq. (13) ($D_{\min}$ is inversely proportional to the per circuit-km transmission cost).

6. Conclusion

Among installation costs of SPV power plant, the location-dependent costs are increasing in share to total installation costs, since the hardware costs are decreasing tremendously. The economic feasibility of SPV power plants depends on the reduction of location-dependent SPV installation costs. Geolocation techniques that exist, for locating SPV installation sites, cannot consider the geospatial socio-economic factors that affect the location-dependent costs spatially. Using a MUFSP model, the factors that cause the spatial nature of location-dependent costs for SPV were studied in a 2500 km^2 suburban region of Kolkata city, India, as a case-study. The main factors that could spatially optimize these costs, were also analyzed and deduced.

The location-dependent costs were indeed minimized at specific locations, with the variation around the minima being significantly sharp for defining the global minima (the location-dependent costs increase by 10% with an average 2.6 km deviation and an average 6.7 km deviation from the global minima, in the 11 kV and 66 kV cases, respectively.). Based on selection of substations at the edge of the city and consideration of 11 kV to 66 kV transmission lines, the peak-capacity of SPV plants, at the optima, varied from 4 MW to 257 MW, with larger SPV plants being more economical than smaller ones. But the minima were sharper for smaller capacities. As transmission voltage and distance of substation from city increased, the capacity of SPV plants at the minima also increased. The distance of the minima also varied from 29 km to 48 km from the city center. The important findings were:

a. The primary factor that causes the spatial variation of installation costs in a suburban boundary is the distance from an economic focal point (position of maximum ft^2 land cost) of the city.
b. The variation of the land and transmission costs, in the suburban region, were significantly more than that of labor and supply chain costs.
c. The optima always lie on the extrapolation of a straight line from the focal point to substation.
d. With increasing transmission line voltage and increasing SPV capacity, the optima shift away from the focal point along the line connecting the focal point to substation.
e. The distance of the optima from the economic focal point is mainly influenced by the per unit land cost and the per circuit-km transmission cost.

The biggest advantage this model provides is a spatial, empirical view of cost optimization for SPV planning. An energy planner may utilize this model for geolocating a cost optimized location for SPV plants, while simultaneously balancing the various parameters affecting the various location-dependent costs. This model can also allow large project developers to plan the land-use around a city, even before an SPV plant is constructed. Also, benchmarking policies of SPV costs towards location-dependent costs can be modified according to the optimization idea presented in this paper. This model shows how spatial social characteristics are important in renewable energy planning for a city.

While this study has been tested on the Indian scenario for Kolkata city, future studies can focus on other cities/countries with different socio-economics, and validate whether the optimized location for a suburban SPV plant lies on the line connecting an economic focal point and a substation. A major limitation of this model may be the restriction to suburban cases, which future studies can expand upon to other geographical areas.

CRediT authorship contribution statement

Soumya Basu: Conceptualization, Methodology, Software, Validation, Formal analysis, Investigation, Resources, Writing – original draft, Visualization. **Takaya Ogawa:** Conceptualization, Writing – Review & Editing, Investigation, Methodology. **Hideyuki**

Table B.1
Model 1 Hedonic test.

Variables	Reg. coefficient	Standard error	*T*-Statistic	*P*-Value
Intercept	9.601	0.609	15.73	0.000
PD	−13.65	6.085	−2.244	0.026
SR	0.327	0.330	0.993	0.322
LR	−0.255	0.555	−0.459	0.646
ER	−0.389	0.498	−0.780	0.436
YPR	−8.398	1.802	−4.659	0.000
HD	34.89	28.85	1.209	0.228
D_{cbd}	−0.207	0.013	−15.93	0.000
Pearson R		0.845		
R – Square		0.714		
Significant - F		0.000		

Table B.2
Model 2 Hedonic test.

Variables	Reg. coefficient	Standard error	*T*-Statistic	*P*-Value
Intercept	10.46	0.540	19.34	0.000
PD	−4.914	1.466	−3.351	0.001
YPR	−6.677	1.752	−3.809	0.000
FLR	−0.291	0.464	−0.627	0.531
FER	0.190	0.306	0.621	0.535
PPH	−0.197	0.059	−3.335	0.001
D_{cbd}	−0.216	0.013	−16.01	0.000
Pearson R		0.853		
R – Square		0.728		
Significant - F		0.000		

Table B.3
Model 3 Hedonic test.

Variables	Reg. coefficient	Standard error	*T*-Statistic	*P*-Value
Intercept	10.17	0.434	23.42	0.000
PD	−4.439	1.459	−3.041	0.002
YPR	−6.111	1.421	−4.300	0.000
PPH	−0.176	0.063	−2.753	0.006
F-MLR	−0.255	0.334	−0.761	0.447
F-MER	0.440	0.247	1.777	0.077
D_{cbd}	−0.213	0.014	−15.23	0.000
Pearson R		0.856		
R – Square		0.733		
Significant - F		0.000		

Table B.4
Model 4 Hedonic test.

Variables	Reg. coefficient	Standard error	*T*-Statistic	*P*-Value
Intercept	10.41	0.246	42.16	0.000
PD	−4.579	1.424	−3.215	0.002
YPR	−5.291	1.449	−3.650	0.000
PPH	−0.228	0.058	−3.943	0.000
D_{cbd}	−0.147	0.033	−4.441	0.000
TT	−0.0181	0.007	−2.352	0.020
Pearson R		0.859079532		
R – Square		0.738017643		
Significant - F		1.48286E−37		

Table B.5
Model 5 Hedonic test.

Variables	Reg. coefficient	Standard error	*T*-Statistic	*P*-Value
Intercept	9.945	0.255	38.97	0.000
PD	−3.980	1.331	−2.990	0.003
YPR	−4.112	1.410	−2.917	0.0041
PPH	−0.152	0.057	−2.689	0.008
D_{cbd}	−0.069	0.035	−1.970	0.051
TT	−0.003	0.008	−0.435	0.664
BT	−0.011	0.004	−3.161	0.002
TRT	−0.004	0.003	−1.334	0.184
Pearson R		0.881		
R – Square		0.776		
Significant - F		0.000		

Okumura: Visualization, Writing – review & editing, Investigation, Methodology. **Keiichi N. Ishihara:** Supervision, Conceptualization, Methodology, Validation, Investigation, Writing – review & editing, Visualization, Project Administration.

Declaration of competing interest

The authors declare that they have no known competing financial interests or personal relationships that could have appeared to influence the work reported in this paper.

Acknowledgments

The corresponding author, Soumya Basu, would humbly like to thank the Konosuke Matsushita Memorial Foundation Scholarship of the Panasonic Corporation for funding his research at Kyoto University, Japan. We all are, further, grateful for the insightful comments offered by the anonymous peer reviewers at *Energy Reports*. The generosity and expertise of one and all have improved this study in innumerable ways and saved us from many errors; those that inevitably remain are entirely our own responsibility.

Appendix A. Hedonic function variables

The equations that were used to calculate the social variables from the raw census data in Table 3 are given as follows:

a. Population Density (PD) = Population in Ward / Area of Ward in km^2
b. Sex Ratio (SR) = Population (female) / Population (male)
c. Literacy Rate (LR) = Population (literate) / Population in Ward
d. Female Literacy Rate (FLR) = Population (female literate) / Population (female)
e. Female to Male Literacy Ratio (F-MLR) = Population (literate female) / Population (literate male)
f. Employment Rate (ER) = Population (total workers) / Population in Ward
g. Female Employment Rate (FER) = Population (female workers) / Population (female)
h. Female to Male Employment Ratio (F-MER) = Population (female workers) / Population (male workers)
i. Youth Population Ratio (YPR) = Population (0-6) / Population in Ward
j. Household Density (HD) = Total Households in Ward/Area of Ward in km^2
k. People per Household (PPH) = Population in Ward/Total Households in Ward

Appendix B. Hedonic regression test models

Below is an account of all the models that were tested in order to approach the Final resultant Hedonic Land Function. (*Note that a P-value higher than 0.01 rejects the variable*) (see Tables B.1–B.5).

Appendix C. Supplementary data

Supplementary material related to this article can be found online at https://doi.org/10.1016/j.egyr.2021.07.068.

References

Ali, A.M., Mustafa, S.S., Mutlag, A.H., 2016. Design optimization of solar power system with respect to temperature and sun tracking. In: 2016 Al-Sadeq Intl. Conf. on Multidis. in IT and Comm. Sci. and Appl. pp. 1–5. http://dx.doi.org/10.1109/AIC-MITCSA.2016.7759956.

Amjad, F., Shah, L.A., 2020. Identification and assessment of sites for solar farms development using GIS and density based clustering technique- a case of Pakistan. Renew. Energy 155, 761–769. http://dx.doi.org/10.1016/j.renene.2020.03.083.

Asim, N., Sopian, K., Ahmadi, S., Saeedfar, K., Alghoul, M.A., Saadatian, O., Zaidi, S.H., 2012. A review on the role of materials science in solar cells. Renew. Sustain. Energy Rev. 16 (8), 5834–5847. http://dx.doi.org/10.1016/j.rser.2012.06.004.

Banerjee, B., Islam, S.M., 2011. Reliability based optimum location of distributed generation. Intl. J. Elec. Power Energy Sys. 33 (8), 1470–1478. http://dx.doi.org/10.1016/j.ijepes.2011.06.029.

Bourassa, S.C., Hoesli, M., Scognamiglio, D., Zhang, S., 2011. Land leverage and house prices. Reg. Sci. Urban Econ. 41 (2), 134–144. http://dx.doi.org/10.1016/j.regsciurbeco.2010.11.002.

Campbell, M., Blunden, J., Smeloff, E., Aschenbrenner, P., 2009. Minimizing utility-scale PV power plant LCOE through the use of high capacity factor configurations. In: 34*th* IEEE Photovoltaic Specialists Conference, 7-12 Sept. http://dx.doi.org/10.1109/PVSC.2009.5411650.

CERC, 2010. Explanatory Memorandum for Benchmark Capital Cost Norms for Solar PV Power Projects and Solar Thermal Power Projects. Central Electricity Regulatory Commission, p. 2010, https://cercind.gov.in/2010/ORDER/Sept10/Explanatory_Memo_for_Project_cost_for_solar_PV_{and}_Solar_thermal_2011-12_255-2010.pdf.

Chakraborty, S., Sadhu, P.K., Pal, N., 2015. Technical mapping of solar PV for ISM-an approach toward green campus. Ene. Sci. Eng. 3 (3), 196–206. http://dx.doi.org/10.1002/ese3.65.

Chandel, M., Agrawal, G.D., Mathur, S., Mathur, A., 2014. Techno-economic analysis of solar photovoltaic power plant for garment zone of Jaipur city. Case Stud. Therm. Eng. 2, 1–7. http://dx.doi.org/10.1016/j.csite.2013.10.002.

Chang, C.T., 2015. Multi-choice goal programming model for the optimal location of renewable energy facilities. Renew. Sustain. Energy Rev. 41, 379–389. http://dx.doi.org/10.1016/j.rser.2014.08.055.

Charabi, Y., Gastli, A., 2011. PV site suitability analysis using GIS-based spatial fuzzy multi-criteria evaluation. Renew. Energy 36 (9), 2554–2561. http://dx.doi.org/10.1016/j.renene.2010.10.037.

Darling, S.B., You, F., Veselka, T., Velosa, A., 2011. Assumptions and the levelized cost of energy for photovoltaics. Energy Environ. Sci. 4, 3133–3139. http://dx.doi.org/10.1039/c0ee00698j.

Das, R., Akay, B., Singla, R.K., Singh, K., 2015. Application of artificial bee colony algorithm for inverse modelling of a solar collector. Inverse Prob. Sci. Eng. 25 (6), 887–908. http://dx.doi.org/10.1080/17415977.2016.1209748.

Davis, M.A., Heathcote, J., 2007. The price and quantity of residential land in the United States. J. Mon. Econ. 54 (8), 2595–2620. http://dx.doi.org/10.1016/j.jmoneco.2007.06.023.

Davis, M.A., Palumbo, M.G., 2008. The price of residential land in large U.S. cities. J. Urban Econ. 63 (1), 352–384. http://dx.doi.org/10.1016/j.jue.2007.02.003.

Diab, A.A.Z., Mohamed, M.A., Al-Sumaiti, A., Sultan, H., Mossa, M., 2021. A novel hybrid optimization algorithm for maximum power point tracking of partially shaded photovoltaic systems. In: Adv. Tech. Solar PV Ene. Sys. Green Ene. & Tech. Springer, p. 201. http://dx.doi.org/10.1007/978-3-030-64565-6_7.

El-Shimy, M., 2012. Analysis of levelized cost of energy (LCOE) and grid parity for utility-scale photovoltaic generation systems. In: 15th International Middle East Power Systems Conference. http://dx.doi.org/10.13140/RG.2.2.10311.29603.

Franklin, J.P., Waddell, P., 2003. A hedonic regression of home prices in king county, washington, using activity-specific accessibility measures. Transp. Res. Board Annu. Meet. http://www.ce.umn.edu/levinson/pa8202/Waddell%20-%20Hedonic.pdf.

Fu, R., Feldman, D., Margolis, R., 2018. U.S. Solar Photovoltaic System Cost Benchmark: Q1 2018. National Renewable Energy Laboratory, https://www.nrel.gov/docs/fy19osti/72399.pdf.

Gouldson, A., Kerr, N., Mcanulla, F., Hall, S., Colenbrander, S., Sudmant, A., Roy, J., Sarkar, S., Ghatak, A., Chakravarty, D., Ganguly, D., 2014. The Economics of Low Carbon Cities: Kolkata, India. University of Leeds, https://www.researchgate.net/publication/270339682_The_Economics_of_Low_Carbon_Cities_Kolkata_India.

Guaita-Pradas, I., Marques-Perez, I., Gallego, A., 2019. Analyzing territory for the sustainable development of solar photovoltaic power using GIS databases. Environ. Monit. Assess 191, #764. http://dx.doi.org/10.1007/s10661-019-7871-8.

Haaren, R.V., Fthenakis, V., 2011. GIS-based wind farm site selection using spatial multi-criteria analysis (SMCA): Evaluating the case for New York State. Renew. Sustain. Energy Rev. 15 (7), 3332–3340. http://dx.doi.org/10.1016/j.rser.2011.04.010.

Helioscart, 2020. Commonly used ACSRs in India. https://medium.com/@helioscart/commonly-used-acsr-conductors-in-india-5930fae4585.

Höller, R., Gudopp, D., Leschinsky, T., 2019. Solar PV Cost Reduction Potential in Japan. http://dx.doi.org/10.20944/preprints201904.0065.v1, Preprints.

IRENA, 2014. Solar power spatial planning techniques. IRENA Glob. Atlas. https://www.irena.org/-/media/Files/IRENA/Agency/Events/2014/Jul/15/9_Solar_power_spatial_planning_techniques_Arusha_Tanzania.pdf?la=en&hash=F98313D5ADB4702FC910B94586C73AD60FA45FDE.

IRENA, 2019. Renewable energy capacity statistics 2019. Int. Renew. Energy Agency https://www.irena.org/-/media/Files/IRENA/Agency/Publication/2019/Mar/IRENA_RE_Capacity_Statistics_2019.pdf.

Janke, J.R., 2010. Multicriteria GIS modeling of wind and solar farms in colorado. Ren. Ene. 35 (10), 2228–2234. http://dx.doi.org/10.1016/j.renene.2010.03.014.

Joyce, K., 2012. Optimizing PV Plant Design To Achieve a Low Levelized Cost of Energy. Black & Veatch, Power-Gen International.

Kain, J.F., Quigley, J.M., 1970. Measuring the value of house quality. J. Amer. Stat. Assn. 65 (330), 532–548, https://www.jstor.org/sTable/2284565.

Katz, L., Rosen, K.T., 1987. The interjurisdictional effects of growth controls on housing prices. J. Law Econ. 30 (1), 149–160. http://dx.doi.org/10.1086/467133.

Lillydahl, J.H., Singell, L.D., 1985. The spatial variation in unemployment and labour force participation rates of male and female workers. Reg. Stud. 19 (5), 459–469. http://dx.doi.org/10.1080/09595238500185451.

McDonald, J.F., McMillen, D.P., 1990. Employment subcenters and land values in a polycentric urban area: The case of Chicago. Env. Plan. A: Econ. Space 22 (12), 1561–1574. http://dx.doi.org/10.1068/a221561.

Meng, F., Zou, Q., Zhang, Z., Wang, B., Ma, H., Abdullah, H.M., Almalaq, A., Mohamed, M.A., 2021. An intelligent hybrid wavelet-adversarial deep model for accurate prediction of solar power generation. Energy Rep. 7, 2155–2164. http://dx.doi.org/10.1016/j.egyr.2021.04.019.

Mondal, B., Bolui, G., Chakraborti, S., 2018. Estimation of spatial association between housing price and local environmental amenities in Kolkata, India using hedonic local regression. Pap. App. Geog. 4 (3), 274–291. http://dx.doi.org/10.1080/23754931.2018.1446354.

Morris, J., Calhoun, K., Goodman, J., Seif, D., 2014. Reducing solar PV soft costs: A focus on installation labor. In: 2014 IEEE 40th PV Spec. Conf (PVSC). pp. 3356–3361. http://dx.doi.org/10.1109/PVSC.2014.6925654.

Mostafa, M., Abdullah, H.M., Mohamed, M.A., 2020. Modeling and experimental investigation of solar stills for enhancing water desalination process. IEEE Access 8, 219457-219472. http://dx.doi.org/10.1109/ACCESS.2020.3038934.

Oguz, E., Şentürk, A.E., 2019. Selection of the most sustainable renewable energy system for bozcaada Island: Wind vs. Photovoltaic. Sustain 11, 4098–4131. http://dx.doi.org/10.3390/su11154098.

O'Shaughnessy, E., Nemet, G.F., Pless, J., Margolis, R., 2019. Addressing the soft cost challenge in U.S. small-scale solar PV system pricing. Ene. Pol. 134, #110956. http://dx.doi.org/10.1016/j.enpol.2019.110956.

Ottensmann, J.R., Payton, S., Man, J., 2008. Urban location and housing prices within a hedonic model. J. Reg. Ana. Pol. 28 (1), 19–35. http://dx.doi.org/10.22004/ag.econ.132338.

Ozcan, O., Ersoz, F., 2019. Project and cost-based evaluation of solar energy performance in three different geographical regions of Turkey: Investment analysis application. Eng. Sci. Tech. Int. J. 22 (4), 1098–1106. http://dx.doi.org/10.1016/j.jestch.2019.04.001.

Padmanathan, K., Govindarajan, U., Ramachandaramurthy, V.K., T., S.O.S., 2017. Multiple criteria decision making (MCDM) based economic analysis of solar PV system with respect to performance investigation for Indian market. Sustainability 9 (5), 820–839. http://dx.doi.org/10.3390/su9050820.

REI, 2016. 日本とドイツにおける太陽光発電のコスト比較, https://www.renewable-ei.org/images/pdf/20160113/JREF_Japan_Germany_solarpower_costcomparison.pdf.

Reta-Hernandez, M., 2006. Chapter 13: Transmission Line Parameters. Universidad Autonoma de Zacatecas, Taylor and Francis Group LLC Publication, https://www.unioviedo.es/pcasielles/uploads/proyectantes/cosas_lineas.pdf.

Rocha, M.S.D.B., Ponczek, V., 2011. The effects of adult literacy on earnings and employment. Econ. Educ. Rev. 30 (4), 755–764. http://dx.doi.org/10.1016/j.econedurev.2011.03.005.

Rumbayan, M., Nagasaka, K., 2012. Prioritization decision for renewable energy development using analytic hierarchy process and geographic information system. In: The 2012 International Conference on Advanced Mechatronic Systems. pp. 36–41, https://ieeexplore.ieee.org/document/6329677.

San Cristóbal, J.R., 2012. A goal programming model for the optimal mix and location of renewable energy plants in the north of Spain. Renew. Sustain. Energy Rev. 16 (7), 4461–4464. http://dx.doi.org/10.1016/j.rser.2012.04.039.

Siali, M., Flazi, S., Stambouli, A.B., Fergani, S., 2016. Optimization of the investment cost of solar based grid. Renew. Energy 97, 169–176. http://dx.doi.org/10.1016/j.renene.2016.05.077.

Singh, G., Das, R., 2020. Comparative assessment of different air-conditioning systems for nearly/net zero-energy buildings. Int. J. Ene. Res. 44 (5), 3526–3546. http://dx.doi.org/10.1002/er.5065.

Sun, Y., Hof, A., Wang, R., Liu, J., Lin, Y., Yang, D., 2013. GIS-based approach for potential analysis of solar PV generation at the regional scale: A case study of fujian province. Ene. Pol. 58, 248–259. http://dx.doi.org/10.1016/j.enpol.2013.03.002.

Tang, J., Huo, Z., Brittman, S., Gao, H., Yang, P., 2011. Solution-processed core–shell nanowires for efficient photovoltaic cells. Nat. Nanotech. 6, 568–572. http://dx.doi.org/10.1038/nnano.2011.139.

Tillmann, P., Jäger, K., Becker, C., 2019. Minimizing the levelized cost of electricity for bifacial solar panel arrays using Bayesian optimization. Appl. Phys. Cornell University, https://arxiv.org/abs/1909.01660v1.

TSERC, 2018. Information on Fixed Cost Estimates. Telengana State Electricity Regulatory Commission, https://www.tssouthernpower.com/ShowProperty/CP_CM_REPO/Pages/TS%20-%20iPASS/InfoFixedCostEstimates.

UERC, 2019. Uttarakhand Electricity Regulatory Commission. Petition (18) of 2019 (Suo-Moto), http://www.uerc.gov.in/orderspetitions/orders/Misc/2019/june19/Order%20dt.%2007.06.19%20on%20benchmark%20cost.pdf.

UPPTCL, 2020. A guideline of ACSR conductors of India. https://upenergy.in/upptcl/en/article/conductors-for-trans.

Wu, Y., Geng, S., 2014. Multi-criteria decision making on selection of solar–wind hybrid power station location: A case of China. Energy Convers. Manage. 81, 527–533. http://dx.doi.org/10.1016/j.enconman.2014.02.056.

Zhang, F., Deng, H., Margolis, R., Su, J., 2015. Analysis of distributed-generation photovoltaic deployment, installation time and cost, market barriers, and policies in China. Energy Policy 81, 43–55. http://dx.doi.org/10.1016/j.enpol.2015.02.010.